

# Significant Improvement of Electrochemical Performance of Ni-rich Cathode Material by Polyethylene Coating

Byeong-Chan Jang and Jong-Tae Son\*

Department of Nano-Polymer Science & Engineering, Korea National University of Transportation Chungju,  
Chungbuk 380-702, Republic of Korea

Received: March 27, 2016, Accepted: July 04, 2016, Available online: August 15, 2016

**Abstract:** We attempted to use polyethylene (PE) to coat the surface of the cathode material in order to suppress these unnecessary reaction, and the results obtained via electrochemical impedance spectroscopy (EIS) suggest the growth of the SEI resistance and charge transfer resistance was suppressed in the samples consisting of 0.1 wt% PE-coated  $\text{Li}[(\text{Ni}_{0.6}\text{Co}_{0.1}\text{Mn}_{0.3})_{0.36}(\text{Ni}_{0.80}\text{Co}_{0.15}\text{Al}_{0.05})_{0.64}]\text{O}_2$  (NCS). The initial discharge capacity of the coated material was of  $190.56 \text{ mAhg}^{-1}$  at 0.1 C between 3.0 and 4.3 V, and 94.6 % of this capacity was retained after 30 cycles. A notable effect of the PE coating, is that the resulting exothermic temperature appears at approximately 258.1 °C, which is higher than that for bare NCS at 249.3 °C.

**Keywords:** Lithium ion battery; Cathode material; Co-precipitation; Polymer coating; Polyethylene(PE)

## 1. INTRODUCTION

Ni-rich  $\text{LiNi}_{1-x-y}\text{Co}_x\text{Mn}_y\text{O}_2$  cathode materials have attracted an increasing amount of interest due to their high capacity, relatively low cost, and low toxicity when compared to  $\text{LiCoO}_2$ . However, Ni-rich cathode materials generally have layered structure that is susceptible to structural degradation from a layered phase to a spinel-like phase and rock-salt phase when cycling and when subjected to elevated temperature [1, 2]. The migration of the transition metal(TM) ions into the lithium layer during charging and discharging leads to the transformation from a layered phase to a spinel phase and this transformation can be intensified when cycling occurs in the presence of high-temperatures and voltages due to the increase in the number of vacant Li sites during full delithiation and diffusion of TM ions. The phase transitions due to the migration of TM-ions are characterized by changes in the lattice constants and in volume, since oxygen is released from the lattice. Such results can lead to thermal and structural instability [3]. The Ni-rich cathode materials are commonly prepared using a general co-precipitation method and are composed of round-shape secondary particles with many aggregated micrometer-sized primary particles (grains). Since all primary particles have different crystallographic orientation and slip planes, the anisotropic expansion or

contraction in the lattice volume between the grains during lithium intercalation or deintercalation results in microcracks that act as new reaction sites for the electrolytes, which in turn leads to electrical disconnection between the grains. The decomposition products of the electrolyte from a new solid electrolyte interface (SEI) layer, along the active surface of the primary particles (grains) that develop due to the microcracks. The SEI layers on the surface of the grains inhibit the electron and lithium transport through the grain–electrolyte interface, thus diminishing the electrical performance of the electrolyte [4, 5]. To address the structural and thermal instability of the Ni-rich cathode materials, researchers have used inorganic materials such as  $\text{Al}_2\text{O}_3$ ,  $\text{ZrO}_2$ ,  $\text{AlPO}_4$ , and  $\text{AlF}_3$  to modify the surfaces [6-8]. Although inorganic coatings have been observed to suppress the interfacial side reactions, the inorganic substances are discontinuously deposited on the cathode materials and also remain as an ionically/electronically resistive layer. As a consequence, the Faradaic reaction kinetics at the cathode material-liquid electrolyte interface can be impaired, negating the benefits purportedly achieved by applying the inorganic coatings. Another disadvantaged is that coating process is complex. The surface of cathode materials can be modified with a conductive polymer to benefit from the delivery of the original capacity without a reduction in the amount of electrochemically active element in the parent cathode materials. The conductive polymer coating layer effectively suppresses the formation of the SEI film and the HF

\*To whom correspondence should be addressed: Email: jt1234@ut.ac.kr  
Phone:

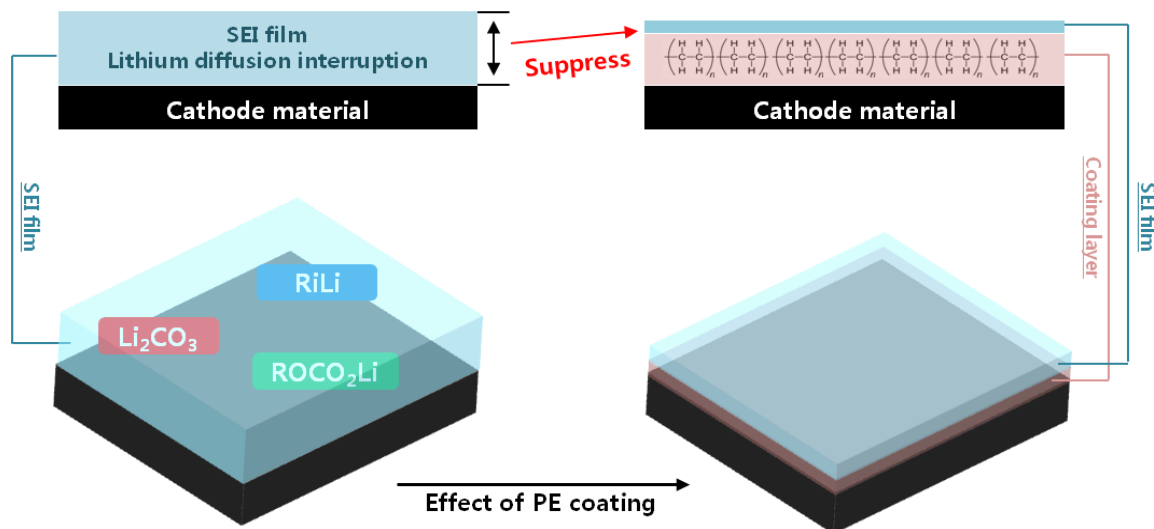


Figure 1. The schematic diagram of bare and PE coated NCS particles.

attack by blocking the contact between the electrolyte and the cathode material. In addition, D.W. Kim and co-workers have reported on simple coating methods [9]. However, the conductive polymer carries a high price, which limits its applicability for use with cathode materials. Polyethylene (PE) is one of the most attractive coating materials that can be used to solve these problems. It can be obtained low cost, and it possesses a high thermal stability and flexibility. Two unnecessary surface reactions contribute to the deterioration of the electrochemical properties of lithium secondary batteries. The first is the formation of a SEI film on the surface of the cathode material, and the second is a HF attack by chemical side reactions. To the best of our knowledge, no reports have been published on PE coated cathode materials to assess the improvement electrochemical properties. In this study, we synthesized Ni-rich  $\text{LiNi}_{1-x-y}\text{Co}_x\text{Mn}_y\text{O}_2$  cathode materials with a high discharge capacity and modified by coating with PE polymer contain coating layer to improve their electrochemical performance. Scanning Electron Microscopy (SEM), Atomic Force Microscopy (AFM), Transmission Electron Microscope (TEM), Differential Scanning Calorimetry (DSC), and electrochemical tests were performed to assess effects of this new approach.

## 2. EXPERIMENTAL

The  $[(\text{Ni}_{0.6}\text{Co}_{0.1}\text{Mn}_{0.3})_{0.36}(\text{Ni}_{0.85}\text{Co}_{0.15})_{0.64}](\text{OH})_2$  precursor was synthesized via co-precipitation. An aqueous solution of  $\text{NiSO}_4 \cdot 6\text{H}_2\text{O}$ ,  $\text{CoSO}_4 \cdot 7\text{H}_2\text{O}$  and  $\text{MnSO}_4 \cdot \text{H}_2\text{O}$  with a concentration of 1 M was pumped into 4 L tank reactor that was continuously stirred under an  $\text{N}_2$  atmosphere. At the same time,  $\text{NaOH}$  (2 M) solution and  $\text{NH}_4\text{OH}$  solution were separately fed into the reactor. During the co-precipitation reaction, the newly formed particles grew into spherical particles under vigorous stirring. In order to construct a core-shell material with a  $[(\text{Ni}_{0.6}\text{Co}_{0.1}\text{Mn}_{0.3})_{0.36}(\text{Ni}_{0.85}\text{Co}_{0.15})_{0.64}](\text{OH})_2$  composition, the  $\text{Ni}_{0.6}\text{Co}_{0.1}\text{Mn}_{0.3}(\text{OH})_2$  product was continuously mixed with the solution containing metal compounds (cationic ratio of Ni:Co = 85:15). The resulting,  $[(\text{Ni}_{0.6}\text{Co}_{0.1}\text{Mn}_{0.3})_{0.36}(\text{Ni}_{0.85}\text{Co}_{0.15})_{0.64}](\text{OH})_2$  particles were then

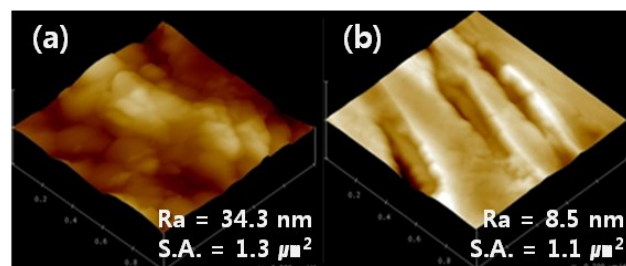


Figure 2. AFM analysis of (a) bare and (b) 0.1 wt% PE coated NCS particles.

filtered, washed, and dried in air or in a vacuum. The core precursors and  $\text{LiOH} \cdot \text{H}_2\text{O}$  were mixed at room temperature for 1 hour, and the core shell precursor,  $\text{LiOH} \cdot \text{H}_2\text{O}$  and  $\text{Al}(\text{OH})_3 \cdot \text{H}_2\text{O}$  were mixed under the same conditions. The mixed powder was calcined at  $800^\circ\text{C}$  for 24 hours under an  $\text{O}_2$  flow. PE powder (Aldrich) was dispersed in xylene at a concentration of 0.1 wt%, the NCS powders were immersed in the polymer solution, and the mixture was stirred at  $60^\circ\text{C}$  for 4h to induce surface coating of the NCM powders. The mixed solution was filtered and then calcined at  $150^\circ\text{C}$  for 12 h to obtain the surface coated NCS powders. The samples were subjected to scanning electron microscopy (SEM QUANTA 300, JEOL) before and after coating; the elemental distribution on the surface of the coated NCS particles was examined using energy dispersive X-ray spectroscopy (EDS); and the electrochemical performance was measured using a CR2032 coin-type cell. The cathode was fabricated by blending the active material, super-P carbon, and binder (8:1:1) in N-methyl-2-pyrrolodone. The mixed slurry was cast uniformly on a thin aluminum foil substrate and was dried in a vacuum for 12 h at  $120^\circ\text{C}$ . A lithium metal foil was used as the anode, a polypropylene micro-porous film was used as the separator, and the electrolyte was consisted of 1 M  $\text{LiPF}_6$  in a 3:7 (v/v) mixture of ethylene carbonate (EC) diethyl car-

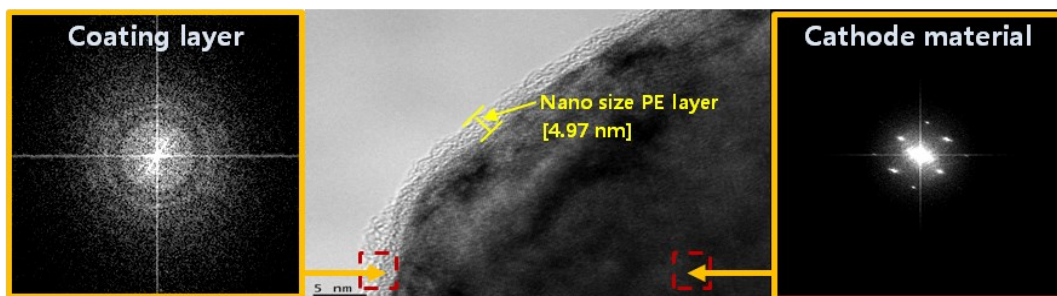


Figure 3. The TEM analysis of bare and 0.1 wt% PE coated NCS particles.

bonate(DEC). Finally, the cells were assembled in an argon-filled glove box. Electrochemical tests were performed between 3.0 and 4.3 V. AC impedance measurements of the Li/NCS cells were performed in SOC (state of charge = 0) using a Solatron 1287 electrochemical interface over the frequency range from 1 Hz to 155 Hz with an amplitude of 10  $\mu$ A.

### 3. RESULTS AND DISCUSSION

#### 3.1. Surface analysis (AFM, TEM)

The effects of the PE coating layers and the interfacial side reactions between the NCS and the liquid electrolytes are schematically illustrated in Fig. 1. The solid electrolyte interphase (SEI) film forms at the interface between the cathode material and the electrolyte during the initial charge process [10]. The oxygen is generated during the reduction of  $\text{Ni}^{4+}$  and oxygen that reacts with the electrolyte to form the SEI film composed of  $\text{Li}_2\text{CO}_3$ ,  $\text{ROLi}$ ,  $\text{ROCO}_2\text{Li}$  [10, 11]. The SEI film causes deterioration in the electrochemical properties since it prevents the diffusion of lithium. However, the PE coating layer suppresses the oxygen emission from the NCS cathode material, and therefore, it is possible for the electrochemical properties to be maintained by suppressing the formation of the SEI film. The change in the surface of the cathode material resulting from the PE coating were observed by conducting a AFM analysis on bare, 0.1 wt% PE-coated NCS particles, as seen in Fig. 2. When compared to bare NCS particles, the surface of 0.1 wt% PE-coated NCS particle were more smooth. The results of roughness average (Ra) were measured, and the Ra of 0.1 wt% PE coated NCS particle decreased from 34.3 nm to 8.5 nm. The surface area (S.A.) decreased from  $1.3 \mu\text{m}^2$  to  $1.1 \mu\text{m}^2$  because the PE coating layer is present between the gap of the primary particles. The decrease in the Ra and S.A. is useful because this reduce the contact area with the electrolyte which can be the site of the HF attack. Therefore, it is possible for the cycle characteristics to improve by suppressing the elution of the transition metal [12-14]. The TEM images of 0.1 wt% PE coated NCS particles confirm the existence of a coating layer. The edge of the 0.1 wt% PE-coated NCS particle is covered with a thin layer (average thickness = 4.97 nm) that is uniformly dispersed. The selected area electron diffraction (SAED) patterns obtained from PE coating layer and NCS cathode material are shown in the left and right insets of Fig. 3, respectively. The SAED pattern corresponding to the PE coating layer (left side) exhibits a hollow ring pattern without bright spots, indicating that the coating layer consisted of disordered polymer materials. The

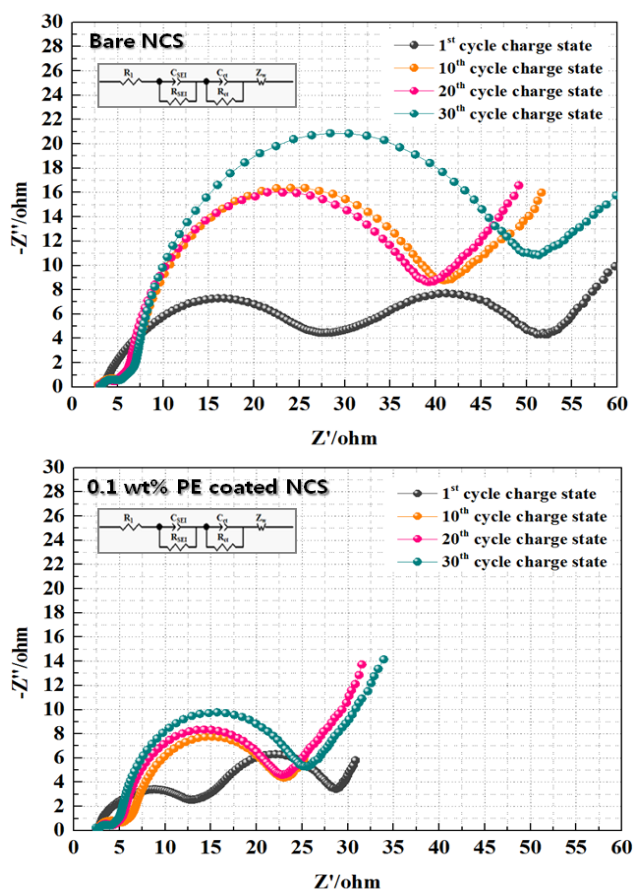


Figure 4. Nyquist plots of bare and 0.1 wt% PE coated NCS electrodes in the charge state of 4.3 V.

image in the right inset shows some bright spot patterns, which is typical for crystalline NCS cathode material. Thus, these results provide conclusive evidence that the primary NCS particles are uniformly coated by the nano sized polymer layer [15, 16].

#### 3.2. Electrochemical impedance spectroscopy (EIS) test

Electrochemical impedance spectroscopy (EIS) can be used to investigate the kinetic process of lithium intercalation/deintercalation into electrodes. Fig. 4 shows the Nyquist plot

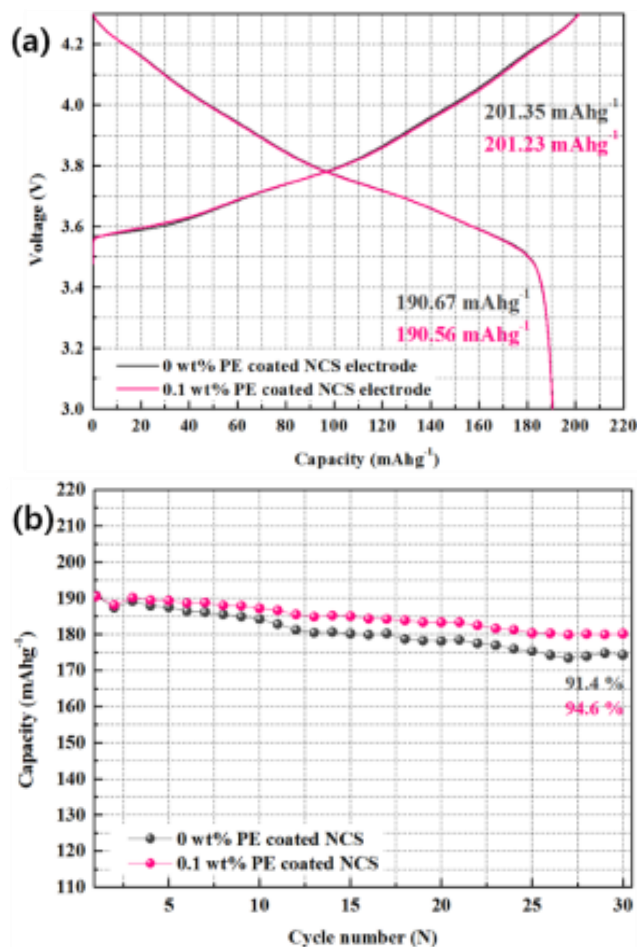


Figure 5. (a) Initial charge & discharge curves and (b) cycle performance of bare and 0.1 wt% PE-coated NCS electrodes at a current density of 17 mA/g in a voltage range from 3.0 to 4.3 V.

of the bare and 0.1 wt% PE coated NCS electrodes during 30<sup>th</sup> cycle performance in the charge state of 4.3 V. The high-frequency semicircle is attributed to the resistance of the solid electrolyte interphase (SEI) film (R<sub>SEI</sub>), and the second semicircle appearing at lower frequency is associated with the charge transfer resistance (R<sub>ct</sub>) [17, 18]. Table 1 shows the R<sub>SEI</sub> and the R<sub>ct</sub> of bare and 0.1 wt% PE coated NCS electrodes during the 30<sup>th</sup> cycle in a charge state of 4.3 V. R<sub>SEI</sub> decreases rapidly after the first cycle, which

Table 1. Fitted impedance parameters of bare and 0.1 wt% PE coated NCS electrodes during 30<sup>th</sup> cycle performance.

	0 wt% PE coated NCS		0.1 wt% PE coated NCS	
	R <sub>SEI</sub> (Ω)	R <sub>ct</sub> (Ω)	R <sub>SEI</sub> (Ω)	R <sub>ct</sub> (Ω)
1 <sup>st</sup> cycle	24.2	24.3	10.3	15.8
10 <sup>th</sup> cycle	2.2	35.8	2.7	17.8
20 <sup>th</sup> cycle	2.2	35.9	1.8	18.5
30 <sup>th</sup> cycle	2.0	46.2	1.5	21.2

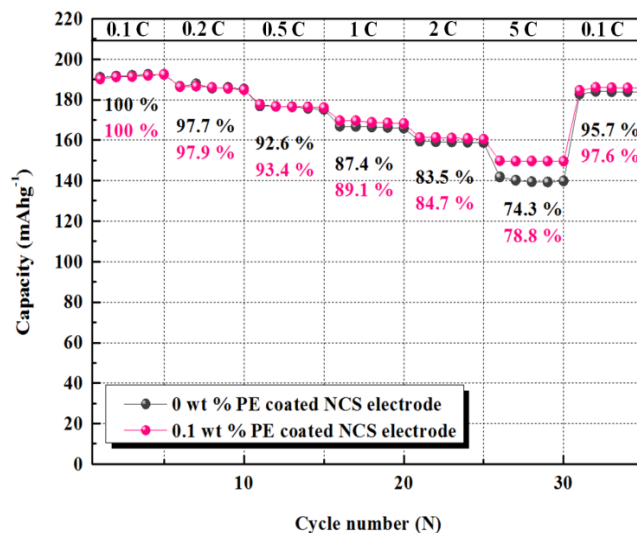


Figure 6. Rate capability curves for bare and 0.1 wt% PE-coated NCS electrodes in the voltage range from 3.0 to 4.3 V at 0.1, 0.2, 0.5, 1, 2, 5, 0.1 C rate.

means that the SEI film that forms first cycle is stabilized. The results indicate that a higher SEI film resistance that forms during the first cycle shows the high charge transfer resistance, and in the case of the 0.1 wt% PE coating, the increase in R<sub>ct</sub> [18, 19]. On the other hand, the R<sub>ct</sub> for the bare NCS electrode increased significantly from 24.3 Ω to 46.2 Ω. These results indicate that the 0.1 wt% PE coated NCS electrodes can offer improvements in the electrochemical properties of the cathode materials.

### 3.3. Electrochemical test

Fig. 5(a) shows the initial charge/discharge curves for the bare and 0.1 wt% PE-coated NCS electrodes at a current density of 17 mA/g (0.1 C) from 3.0 to 4.3 V. The initial charge and discharge capacity of the bare NCS electrodes are 201.35 mAhg<sup>-1</sup> and 190.67 mAhg<sup>-1</sup>. In contrast, the 0.1 wt% PE-coated NCS electrodes exhibit an initial charge and discharge capacity of 201.23 mAhg<sup>-1</sup> and 190.56 mAhg<sup>-1</sup>. In the case of the 0.1 wt% PE-coated NCS electrodes, the R<sub>ct</sub> decreases after the initial charge process due to the decrease in R<sub>SEI</sub>. Therefore, the reduction in capacity due to the non-active coating layer is not confirmed.

Fig. 5(b) shows the cycling performance of the bare and 0.1 wt% PE-coated NCS electrode at a current density of 17 mA/g (0.1 C) from 3.0 to 4.3 V. The initial discharge capacity of the 0 wt% PE-coated NCS electrode decreased from 190.67 mAhg<sup>-1</sup> to 174.27 mAhg<sup>-1</sup> by the 30<sup>th</sup> cycle (30<sup>th</sup> cycle efficiency = 91.4 %). The 0.1 wt% PE-coated NCS electrode delivered an initial discharge capacity of 190.56 mAhg<sup>-1</sup> that was reduced to 180.18 mAhg<sup>-1</sup> after the 30<sup>th</sup> cycle (30<sup>th</sup> cycle efficiency = 94.6 %). The cycle efficiency is a result of the suppression of the SEI film and the HF attack. Since the SEI film is suppressed, R<sub>ct</sub> is reduced, so the insertion/extraction of the Li<sup>+</sup> ions occurs more smoothly during the charge and discharge process [19, 20]. Also, the contact area that experiences the HF attack is reduced, resulting in an improvement in the structural stability of the reduced transition metal elution

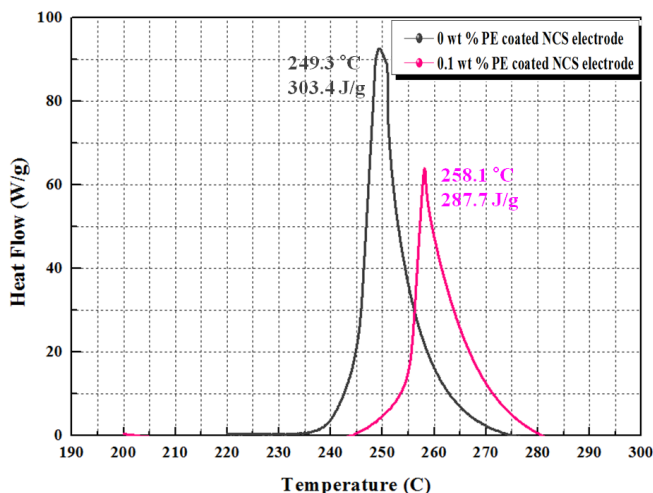


Figure 7. Differential scanning calorimetry (DSC) curves for bare and 0.1 wt% PE-coated NCS electrodes

[21]. Fig. 6 shows the rate capability for bare and 0.1 wt% PE-coated NCS electrodes at various current densities. The 0.1 wt% PE-coated NCS electrodes exhibited a higher capacity efficiency than the bare NCS electrode for every rate, which further demonstrates the improvement in the rate capability. These results suggest that easier lithium intercalation/deintercalation is responsible for reducing the charge transfer resistance [22, 23]. Fig. 7 shows the differential scanning calorimetry (DSC) curves for bare and 0.1 wt% PE-coated NCS materials in a charged state at 4.3 V. The bare NCS material had a large exothermic peak at 249.3 °C, and the reaction released heat of 303.4 J/g. In contrast, the 0.1 wt% PE-coated NCS material had a reaction at a higher temperature of 258.1 °C with a released heat of 287.7 J/g. It is obvious that the thermal stability is remarkably improved by PE coating, which protects reaction the highly oxidized cathode with the electrolyte decomposition [24,25] and thus reduces the exothermic reaction.

#### 4. CONCLUSIONS

The PE coating layer effectively inhibited the formation of the SEI film after a 4.3 V initial charge process. RSEI decreased as a result of the reduction in the SEI film. In addition, the decrease in RSEI improved the lithium intercalation/deintercalation and reduces Rct. These results indicate that the reduction in the initial capacity of the non-active coating layer was not confirmed, and the efficiency improved as 94.6% at the 30<sup>th</sup> cycle. In particular, the DSC analysis revealed that the 0.1 wt% PE-coated NCS material possesses an improved thermal stability through a reduction in the heat generated and an increase in the exothermic peak.

#### 5. ACKNOWLEDGMENTS

Acknowledgments: This study was supported by the granted financial resource from the Ministry of Trade program of the Industry & Energy, Republic of Korea (G02N03620000901) and the Global Excellent Technology Innovation of the Korea Institute of Energy Technology Evaluation and Planning (KETEP).

#### REFERENCES

- [1] M. Guilnard, L. Croguennec, D. Delmas, *Chem. Mater.*, 15, 4476 (2003).
- [2] Z. Lu, J.R. Dahn, *J. Electrochem. Soc.*, 149, A1454 (2002).
- [3] Z. Lu, J.R. Dahn, *J. Electrochem. Soc.*, 149, A815 (2002).
- [4] Y.J. Park, Y.S. Hong, X. Wu, K.S. Ryu, S.H. Chang, *J. Power Sources*, 129, 288 (2004).
- [5] X. Yang, X. Wang, L. Hu, G. Zou, S. Su, Y.S. Bai, H.B. Shu, Q. Wei, B.N. Hu, L. Ge, D. Wang, L. Liu, *J. Power Sources*, 242, 589 (2013).
- [6] Y.K. Sun, S.T. Myung, M.H. Kim, J. Prakash, K. Amine, *J. Am. Chem. Soc.*, 127, 13411 (2005).
- [7] B.C. Park, H.J. Bang, K. Amine, E. Jung, Y.K. Sun, *J. Power Sources*, 174, 658 (2007).
- [8] K.S. Lee, S.T. Myung, Y.K. Sun, *J. Power Sources*, 195, 6-43 (2010).
- [9] H.J. Noh, S.J. Youn, C.S. Yoon, Y.K. Sun, *J. Power Sources*, 233, 121 (2013).
- [10] S.W. Cho, G.O. Kim, J.H. Ju, J.W. Oh, K.S. Ryu, *J. Materials Research Bulletin*, 47, 2830 (2012).
- [11] Y. Qi, Y. Huang, D. Jia, S.J. Bao, Z.P. Guo, *Electrochimica Acta*, 54, 4772 (2009).
- [12] G.H. Kim, J.H. Kim, S.T. Myung, C.S. Yoon, Y.K. Sun, *J. Electrochem. Soc.*, 152, A1707 (2005).
- [13] C. Wu, F. Wu, L. Chen, X. Huang, *Solid State Ionics*, 152, 327 (2002).
- [14] M. Kageyama, D. Li, K. Kobayakawa, Y. Sato, Y.S. Lee, *J. Power Sources*, 157, 494 (2006).
- [15] S.H. Kang, K. Amine, *J. Power Sources*, 146, 654 (2005).
- [16] J.W. Mullin, *Crystallization Butterworths*, London, 1961.
- [17] G.W. Yoo, H.J. Jeon, J.T. Son, *Journal of the Korean electrochemical Society*, 16, 59 (2013).
- [18] R.J. Gummow, M.M. Thackeray, W.I.F. David, S. Hull Mater, *Res. Bull.*, 27, 1992, p.327.
- [19] S.U. Woo, B.C. Park, C.S. Yoon, S.T. Myung, J. Prakash, Y.K. Sun, *J. Electrochem. Soc.*, 154, A649 (2007).
- [20] G.G. Amatucci, N. Pereira, T. Zheng, J. -M. Tarascon, *J. Electrochem. Soc.*, 148, A17 (2001).
- [21] J.R. Dahn, U. von Sacken, C.A. Michal, *Solid State Ionics*, 44, 87 (1990).
- [22] J.N. Reimers, E. Rossn, C.D. Jones, J.R. Dahn, *Solid State Ionics*, 61, 335 (1993).
- [23] M. Zhou, L. Zhao, T. Doi, S. Okada, J. Yamaki, *J. Power Sources*, 195, 4952 (2010).
- [24] M. Zhou, L. Zhao, S. Okada, J. Yamaki, *J. Power Sources*, 196, 8110 (2011).